Title: High level ab initio, DFT, and RRKM calculations for the Unimolecular Decomposition Reaction of Ethylamine

Author: Mansour H. Almatarneh Mohammednoor Altarawneh Raymond A. Poirier Ibrahim A. Saraireh

PII: S1877-7503(14)00026-X
DOI: http://dx.doi.org/doi:10.1016/j.jocs.2014.02.003
Reference: JOCS 261

To appear in:

Received date: 30-10-2013
Revised date: 9-2-2014
Accepted date: 13-2-2014

Please cite this article as: Mansour H. AlmatarnehMohammednoor AltarawnehRaymond A. PoirierIbrahim A. Saraireh High level ab initio, DFT, and RRKM calculations for the Unimolecular Decomposition Reaction of Ethylamine (2014), http://dx.doi.org/10.1016/j.jocs.2014.02.003

High level ab initio, DFT, and RRKM calculations for the Unimolecular Decomposition Reaction of Ethylamine

Mansour H. Almatarneh[1*]; Mohammednoor Altarawneh[2,3]; Raymond A. Poirier[4], Ibrahim A. Saraireh[5]

[1] Department of Chemistry, University of Jordan, Amman 11942, Jordan.

[2]School of Engineering and Information Technology, Murdoch University, Perth, Australia

[3] Chemical Engineering Department, Al-Hussein Bin Talal University, Ma'an, Jordan.

[4] Chemistry Department, Memorial University, St. John's, NL, A1B 3X7, Canada.

[5] Chemistry Department, Al-Hussein Bin Talal University, Ma'an, Jordan.

*Corresponding author:

E-mail: almatarneh@yahoo.com

Tel: +962790182748

Fax: +96265348932

Abstract

Mechanisms for the decomposition reaction of ethylamine, $CH_3CH_2NH_2$, were investigated using ab initio, DFT, and RRKM calculations. Optimized geometries of reactants, transition states, intermediates, and products were determined at HF, MP2, and B3LYP levels of theory using the 6-31G(d) and 6-31+G(d) basis sets. Single point energies were also determined at G3MP2B3 and G3B3 levels of theory. Thermodynamic properties, activation energies, enthalpies and Gibbs energies of activation were calculated for each reaction pathway investigated. Intrinsic reaction coordinate (IRC) analysis was performed to characterize the transition states on the potential energy surface. The conformational change and planarity of the ethylamine moiety along with the twist angle of the amino group about the CN axis are examined. Four pathways for the decomposition reaction of ethylamine were studied. All pathways involve a 1,2-elimination reaction and 1,3-proton shift to produce ethene, ethanimine, ethenamine, and methanimine. All pathways are single-step mechanisms. Elimination of the NH_3 dominates the decomposition behaviour up to 1200 K whereas after this temperature, secession of the C-N gradually holds more importance. While pathways signifying departures of NH_3 and NH_2 exhibit pressure-dependent behaviour, branching ratios for these two channels are generally not influenced by variation in pressure higher than the atmospheric pressure.

1. INTRODUCTION

1,2-Elimination and 1,3-proton shift reactions are of fundamental interest in organic chemistry and are ubiquitous processes in gas-phase chemistry of cationic or anionic species [1-5]. Among these reactions that can undergo the 1,2-elimination and 1,3-proton shift is the decomposition (pyrolysis) of ethylamine (C_2H_7N). Ethylamine (**EA),** also known as ethanamine (IUPAC name), monoethylamine, aminoethane, and 1-aminoethane, is considered as the simplest prototype of primary amines containing C-H, N-H, C-C, and C-N bonds. Thus, the reactions of EA are typical for primary and secondary amines. It is considered to be a weak base and it is widely used in chemical industry and organic synthesis. It is a precursor to many herbicides including atrazine and simazine and is found in rubber products as well.

It is produced on a large scale by combining ethanol and ammonia in the presence of an oxide catalyst [6]. Ethylamine is miscible with virtually all solvents and considered a good solvent for lithium metal, which is used for the reduction of unsaturated organic compounds [7].

A great deal of work has been obtained experimentally [8-31] and theoretically [31-36] for the decomposition of ethylamine and several new species have been positively identified by means of their vibrational spectra analysis. The pioneering study of Taylor [8] pointed out that the decomposition reaction of EA is unimolecular, as some species were not observed. He also found that the decomposition is a homogeneous unimolecular reaction in the range of 500-540 °C and 50-400 *mmHg* [8]. Later, Taylor and Ditman [9] stated that the decomposition reaction at low pressure was heterogeneous, complex and probably involving a chain reaction mechanism. More notably, recent interest in studying the decomposition of the EA molecule stems from the fact that it represents a simple model compound for nitrogen content in biomass. Oxidation and pyrolysis of EA [10, 11] was found to afford nitrogen oxides (NOx), HCN, NH_3 and other nitrogenated species. By simulating ignition delay times and NH_2 concentration time-histories, it was found that the decomposition of the EA molecule proceed with an activation energy of 290 kJ/mol [10].

More recently, Bouchoux et al. [2] studied the unimolecular dissociation of protonated ethylamine $[CH_3CH_2NH_3]^+$ using ab initio calculations and mass spectrometric techniques. They proposed three alkene elimination reaction channels. Several studies have discussed the structure of vinylamine by microwave rotational spectra [12] and ab initio calculations [35]. Vinylamine is a model of enamine protonation which represents ambident-conjugated systems with high nucleophilicity at both the nitrogen and β-carbon atom. Ethylamine binds to metals through its nitrogen lone pair [13]. Recently, Lu et al. [34] studied the reactions of Co^+ with ethylamine using DFT calculations. They proposed six different "classical" N and "nonclassical" ethyl-H attached isomers for the Co^+-ethylamine complexes. The elimination products occur through Co^+ insertion into the N-H, C-C, and R-NH_2 bonds. Ethylamine can be partially dehydrogenated like ethylamine upon heating to yield CH_3CN (acetonitrile) and HCN (in case of methylamine) in the 300-400K temperature range [13-15]. The

thermal decomposition of EA has been studied on several surfaces where CH_4, NH_3, and CH_3CN were detected by spectroscopic methods [13]. Lovas et al. [12] stated that pyrolysis of ethylamine can theoretically follow two stage-cracking routes, which produces nine stable polar species and three non-polar species. They pointed out that the reaction is unimolecular, as some species were not observed by their measurements. They characterized the microwave rotational spectra of vinylamine (CH_2=CH-NH_2) in the gas phase pyrolysis decomposition products of ethylamine. They suggested that vinylamine has a nonpolar equilibrium structure.

In this article, we initially examine the planar and the pyramidal conformation of the C-NH_2 group. Calculations were carried out using different conformers. These conformers represent different orientations of the amine group (-NH_2) with respect to the ethylamine group. In the present paper, we report a theoretical study of mechanisms for the decomposition reaction of ethylamine. We were interested in the first stage-cracking pattern postulated for the decomposition of EA. In addition, to determine whether the decomposition reaction of EA will be unimolecular, as stated in the literature, or bimolecular. The decomposition of ethylamine follows four pathways. The decomposition reaction of ethylamine involves the removal of H_2, NH_3, and CH_4 and formation of ethene, ethanimine, ethenamine, and methanimine by elimination and 1,3-proton shift as summarized in Scheme 1. The goal of this paper is to unravel the reaction mechanism of EA of all possible pathways associated with the observed products using high level ab initio and DFT calculations as well as a comparison of the theoretical results with the experimental findings. This work will shed some new light on the mechanism for reactions of transition-metal ions with primary amines.

Insert Scheme 1

2. Computational Method

All the computations were performed with the Gaussian03 suite of programs [37]. The geometries of all reactants, transition states, intermediates, and products were fully optimized at HF, MP2, and B3LYP [38] levels of theory using the 6-31G(d) basis sets. To further confirm the reliability of the 6-31G(d), the 6-31+G(d) basis set has also been utilized to examine the effect of diffuse functions. We chose the DFT functional which is known to give reliable energetics for such system as confirmed from our previous results [3]. Single point energies were determined at G3MP2, G3MP2B3, and G3B3 levels of theory. The principal reason for employing different levels of theory is to assure that the relative stabilities remain independent of the basis set and are not an artifact of the geometry optimization. The complete reaction pathway for each mechanism discussed in this paper has been verified using Intrinsic Reaction Coordinate (IRC) analysis of all transition states. The last structures of the IRC in both directions were further optimized, in order to positively identify the minima to which each transition state is connected. The transition state between two stable conformers was also located using QST2 (Quadratic Synchronous Transit) and QST3 approach [39]. Vibrational frequency analysis was performed for each stationary point in order to verify that the minima had no imaginary frequency and that transition states had a single imaginary frequency.

The microcanonical Rice-Ramsperger-Kassel-Marcus (RRKM) theory [40] was used to evaluate pressure dependent reaction rate constants, i.e., $k(T,P)$ as implemented in the Chemrate code [41]. This methodology is based on solving the one-dimensional master equation based on the J-distribution of the Boltzmann probability complex. Tunnelling effects are accounted for in these systems using a one-dimensional Eckart functional [42]. Reaction rate constants at the high-pressure limit are fitted to modified Arrhenius equation:

$$k(T) = A\grave{T}^{n} \exp(-E_a / RT)$$

Where A is the pre-exponential factor, Ea is the activation energy, and n is a unitless parameter.

In calculations of reaction rate constants, internal rotation about the C-N bond is treated as a hindered rotor. The three-fold rotational potential is found to entail a barrier of 11.1 kJ/mol with a rotational constant at 271.5 GHz. These values are in excellent agreement with previously reported theoretical predictions [35].

3. Discussion

3.1 The Molecular Structure of Ethylamine

First, we considered and distinguished between a planar and the pyramidal conformation of the C-NH_2 group of ethylamine. The conformations were optimized at the HF, MP2 and B3LYP levels of theory using the 6-31G(d) basis set. Three minima have been found, see Fig. 1. The one with a dihedral angle of 0° corresponds to the *trans* conformer while the other two at ±120° are two equivalent gauche conformers. Therefore, EA has two possible conformers, one being the *trans* conformer where the lone pair of the -NH_2 group is *trans* with respect to the C-C bond, whereas in the *gauche* conformer, the lone pair is *gauche* to the C-C bond [31-32], see Fig. 1.

Insert Fig. 1

Several theoretical and experimental studies [21-28, 31-33] have been carried out to determine the relative stability of the conformational change of EA. The experimental results suggest a pyramidal nitrogen for EA. Earlier results [34,35], and a microwave spectroscopic analysis [12] suggested that EA is non-planar. Radom et al. [28] and Manocha et al. [23] predicted that the *gauche* conformer is more stable than the *trans* conformer. On the other hand, Tsuboi et al. [24] and Durig et al. [25,26] used spectroscopic methods (IR and Raman) in which they stated that *trans* is more stable. Similarly in later studies, Fischer et al. [27] (using microwave spectroscopy), Hamada et al. [21,22] (IR and ED experiments), Zeroka et al. [31,32] (ab initio calculations at MP2/6-31G(d,p)) have pointed out that the *trans* conformer is more stable. Zeroka et al. [31,32] published an exhaustive analysis of the internal and inversion of the amino group in EA where two the conformers were

noted as *trans*- and *gauche*-ethylamine. More recently, Yan et al. [33] suggested that the *trans* is more stable as well. They pointed out that the Boltzmann-weighted abundance of these EA conformers exist as 39% for *trans* and 61% for two equivalent *gauche* conformers.

In this paper, we found that the *trans* conformer is more stable than the *gauche*. However, the difference in energy between them is in the fourth decimal place at all the levels of theory and basis sets used in this paper (For example: -135.179406 and -135.1792954 Hartrees for *trans* and *gauche,* respectively, at B3LYP/6-31G(d) level). It is worth noting that the conformer of EA obtained from the IRC calculations on the TS's was the *gauche* conformer for pathways **A** and **C** and the *trans* conformer in pathways **B** and **D**. The optimized geometry of ethylamine is shown in Fig. 2 along with selected structural parameters. Some selected calculated and experimental structural parameters for ethylamine are given in Table 1. The C-C and C-N bond lengths are 1.535Å and 1.468Å, respectively for *trans*-ethylamine, and 1.528Å and 1.470Å, respectively for gauche-ethylamine. The <CCN angle of the *trans* conformer is 116.1° compared with 110.5° for the *gauche* conformer, see Table 1. It can be concluded that the agreement between our calculated results is very good and coincides with the other calculated and experimental results [2,22,25,31,34]. The C-N bond length and the <CCN angle compare relatively well with those of vinylamine [determined by Lovas et al. [12], in which they suggested that the vinylamine has a nonpolar equilibrium structure where the (C-N) distance is 1.40Å and <CCN is 125°. The R-*trans* structure (reactant structure) was found to be more stable than the R-*gauche* structure by less than 2 kJ/mol; however, the evidence from IRC at different levels of theory seems to favour both conformers. Therefore; R was used in this article to represent the reactant optimized ground state structure, see Fig. 3.

Insert Table 1

Insert Fig. 2

3.2 Reaction Mechanisms for the Decomposition of Ethylamine:

The reactants, transition states, and products for the decomposition reaction of ethylamine are shown in Scheme 1. Four pathways initiated from the four different proton shifts have been investigated. All pathways involve a one-step mechanism. The activation energy, the enthalpy of activation, and Gibbs energy of activation for this reaction at various levels of theory are listed in Table 2.

The geometries for the reactant, transition state, and product involved in all pathways (**A**→**D**) are given in Fig. 3. Their relative energies are given in Fig. 4. The activation energy for pathways **A** is 285 kJ mol^{-1} at G3MP2B3 level of theory, which is the lowest barrier among the other proposed mechanisms. In pathway **A**, one hydrogen transfers, through a 1,3-proton shift, from the methyl group to the amino group to produce CH_2=CH_2 (ethene) and NH_3 (ammonia). It is worth pointing out that the CCN angle is decreased from 110.5° to be 99.9° in the TS. Decreasing the CCN angle results in significant angle strain and thus accounts for the high barrier. The geometries for the reactant, transition state, and product involved in pathway **B** along with their relative energies are given in Fig. 3 and Fig. 4. In this pathway, a 1,3-proton shift occurs in the opposite direction where the proton transfers from the amino group to the methyl group to yield CH_2=NH and CH_4. The activation energy for pathway **B** is 421 kJ mol^{-1} at G3MP2B3 level of theory, see Table 2. This barrier is very high compared to pathway **A**.

The geometries for the reactant, transition state, and product involved in pathway **C** and **D** along with their relative energies are given in Fig. 3 and Fig. 4, respectively. In pathway **C**, a 1,2-elimination of hydrogen occurs at the C-N bond to produce CH_3-CH=NH (ethanimine) and H_2. While in pathway **D**, a 1,2-elimination at the C-C bond yields CH_2=CH-NH_2 (ethenamine) and H_2. The activation energies for pathways **C** and **D** are 547 and 470 kJ mol^{-1} at G3MP2B3 level of theory, respectively, see Table 2. These barriers are also very high compared to pathway **A**. The activation energy for pathway **C** at G3MP2 level was very low because the TS is converted into a reactant-like structure.

Insert Fig. 3 and Fig. 4

Insert Table 2

Table 3 shows the energies, enthalpies, and Gibbs energies for the decomposition reaction of ethylamine in kJ mol^{-1} for pathways **A**, **B**, **C**, and **D**. It can be seen from Table 3 that the decomposition reaction of ethylamaine is endothermic and endergonic (non-spontaneous reaction) at all levels of theory.

Insert Table 3

As we can see, hydrogen abstraction, from C and N atoms, is the most probable primary step in the proposed mechanism for the decomposition reaction. Since C-H and N-H bond strengths are almost equal, it may be assumed that hydrogen abstraction from nitrogen and carbon sites should occur equally. However, the barriers for these mechanisms were different depending on the site where the abstraction occurs as we showed earlier. The Gaussian-n values differ by no more than 9 kJ mol^{-1}. B3LYP/6-31+G(d) are in excellent agreement with the G3MP2B3 value, differing by no more than 10 kJ mol^{-1}.

3.3 High-Pressure Limit Reaction Rate Constant

Thermal rate constants at the high-pressure limit, $k(T)_{uni}$, are obtained by using transition state theory (TST) for pathways **A**, **B**, **C** and **D**. The located transition state structures at the G3MP2B3 level are used to derive modified Arrhenius parameters for the rate constant. These parameters are given in Table 4. For the barrierless fission of the $CH_3CH_2…NH_2$ bond, variational transition state theory (VTST) is used to estimate the reaction rate constant. In this methodology, the rate constant is minimized as a function of temperature at each reaction coordinate, *viz*, the $CH_3CH_2…NH_2$ bond elongation. The implementation of the VTST is well-described in many recent studies.

Insert Table 4

The potential energy surface (PES) for the $CH_3CH_2…NH_2$ bond fission is constructed by performing partial optimization at an interval of 0.1 Å along the reaction coordinate at G3MP2B3. The PES is shown in Fig. 5.

Insert Fig. 5

The transition state is found to occur at a $CH_3CH_2…NH_2$ bond length of 3.800 Å in the temperature interval of 300-1300 K; while it tightens slightly to 3.600 Å when the temperature increases above 1300 K. Modified Arrhenius parameters for pathway **E** are given in Table 4. It is worth noting that the presence of the methyl group in both the reactant and the transition structure of pathway **E** is most likely to diminish to great extent the hindered rotor effect of the methyl group on the calculated rate constant for pathway **E**.

By inspection of the high-pressure rate constants of the five pathways considered, one can see that the unimolecular decomposition of ethylamine is dominated by ammonia expulsion (channel **A**) and fission of the C-N bond (channel **E**). Despite of the sizable difference in the calculated activation energy *Ea* between pathways **A** and **E**, the very late product-like transition structure in pathway **E** has a larger entropy of activation in this channel, and hence larger *A* factor compared to pathway **A**. As a result, rate constants for pathways **A** and **E** are comparable at intermediate temperatures. The experimentally fitted *E*a value of 298 kJ/mol [10] is in relatively good agreement with corresponding calculated *Ea* values for channels **A** (285.7 kJ/mol) and **E** (362.2 kJ/mol)**.**

3.4 Pressure-Dependent Rate Constants and Branching Ratio

By using a shock tube coupled with laser-absorption methods, Sijie et al. [10] found that initial thermal decomposition of EA is controlled by fission of the C-N bond, i.e., channel E. Measuring NH_2 time histories at temperature and pressure ranges of 1223- 1790 K and 1.2 – 2.1 atom yielded a reaction rate constant of for the bimolecular reaction rate constant of ($CH3CH_2NH_2 + M \rightarrow CH_3CH_2 + NH_2 + M$); where M signifies any collided third body:

$$k(T) = 8.9\times10^{18} \exp(\frac{-35\ 809}{T})\ \text{cm}^3\ \text{mol}^{-1}\ \text{s}^{-1}$$

In order to evaluate the contribution of channels **A** and **E** under practical conditions of elevated temperatures and various operational pressures and to compare estimated reactions rate constnats with experimental values, pressure-dependent rate constants; $k(T,P)$ based on the RRKM theory are calculated. The Lennard-Jones (*L-J*) parameters used for ethylamine are σ = 4.7005 Å and κ = 383.05 K [43]. The average step size for energy transfer per collision, $\langle E \rangle_{down}$, is taken to be 800 cm^{-1} in order to provide intermediate collision frequency. Argon is used as a bath gas and an energy size, ΔE, of 10 cm^{-1} is used. Parameters for rate constants for modified Arrhenius parameters for pathways **A** and **E** at 0.01 atm, 1.00 atm and 100.00 atm are given in Table 5.

Insert Table 5

Both channels; **A** and **E** exhibit strong pressure dependency-behaviour. The dependence of the rate constant on pressure for pathway **A** becomes important only at higher temperatures whilst the rate constant for fission of $CH_3CH_2\ldots NH_2$ bond exhibits very strong pressure-dependence even at temperatures as low as 800 K. For example, rate constants for the elimination of NH_3 and the $CH_3CH_2\ldots NH_2$ bond fission channels at 1000 K are smaller than their high-pressure limits by factors of 1.1 and 1.7, respectively.

Branching ratios for pathways **A** and **E** are evaluated based on the modified Arrhenius parameters for $k(T, P)$ given in Table 5. Plots for $K_E / (K_A + K_E)$ are given in Fig. 6.

Insert Fig. 6

In an agreement with experimental finding, channel **E** dominates thermal decomposition of EA at atmospheric pressure starting from a temperature of ~ 1200 K; whereas below this temperatures. NH_3 elimination dominates the decomposition behaviour. However, low operational pressures (i.e., 0.01 atm) favors elimination of NH_3 at the entire temperature range. As given in Fig. 6, the branching ratio of pathway **E** at 100.0 atm coincide with the branching ratio at the high-pressure limit at all temperatures.

The influence of $\langle E \rangle_{down}$ on $k(T,P)$ for pathways **A** and **E** is investigated by evaluating the reaction rate constant for channel **E** at the normal atmospheric pressure at energy transfer rates of 100 cm^{-1}, 400 cm^{-1}, 800 cm^{-1}, and 1200 cm^{-1} ranging from weak to strong collision conditions. Fig. 7 shows reaction rate constant for Channel E for various $\langle E \rangle_{down}$.

Insert Fig. 7

As shown in Fig. 7, deploying $\langle E \rangle_{down}$ values higher than 800 cm^{-1}, yields very comparable values to corresponding values obtained at 800 cm^{-1}. This implies that an optimised value for $\langle E \rangle_{down}$ could be set at 800 cm^{-1}; i.e.; the value that we have utilised to obtain our $k(T,P)$ for channels A and E.

In order to compare our $k(T,P)$ values for channel **E** with corresponding experimental measurements, the experimental rate constant obtained for channel **E** is transformed into unimolecular values and plotted in Fig. 8 alongside our $k(T,P)$ values. Our calculated $k(T,P)$ values are estimated at a pressure of 1.6 atm to account for the low (1.2 atm) and high (2.1 atm) experimental pressure values. Fig. 8 exhibits a reasonable agreement between calculated and experimental values for channel E. The experimental values are higher than corresponding calculated values by factors in the narrow range of 2.38 – 2.41 for the considered temperature interval 1223 – 1790 K.

Insert Fig. 8

4. Conclusions:

The configuration of the C-NH_2 group was examined to distinguish between the planar and pyramidal conformations of the NH_2 group of ethylamine**. EA** has two conformers, one *trans* and two equivalent *gauche* conformers (rotamers) due to the internal rotation of the amino group about the C-N axis. The mechanism for the decomposition reaction of ethylamine was investigated using ab initio, DFT, and RRKM calculations. The IRC analysis was carried out for all transition state structures to obtain the complete reaction pathway. Four pathways for the decomposition reaction were found. This paper reports the first detailed study of possible mechanisms for the decomposition reaction of ethylamine. Values of $k(T,P)$ are estimated for pathways **A** and **E** to simulate conditions encountered in a real combustion/pyrolysis environment. Branching ratios for these two channels are found to change slightly when varying operating pressures and collisions probabilities. Calculated reaction rate constant for channel **E** supports the experimental finding with regard to the predominance of C-N fission at elevated temperatures and moderate pressures.

Acknowledgement. We thank the reviewers for their constructive suggestions on the paper. We gratefully acknowledge the Atlantic Computational Excellence Network (ACEnet) for computer time. R.A.P. is grateful to the Natural Sciences and Engineering Council of Canada (NSERC) for financial support.

Supporting Information Available: Full geometries and energies of all structures for all pathways investigated at all levels of theory discussed in the present paper along with Vibrational frequencies (cm^{-1}) and rotational constants.

References

[1] H. Fujiwara, T. Egawa, S. Konaka, Electron diffraction study of thermal decomposition products of trimethylamine: molecular structure of CH_3-N=CH_2, J. Mol. Struct. 344 (1995) 217–226.

[2] G. Bouchoux, F. Djazi,Gas-Phase Chemistry of Protonated Ethylamine: A Mass Spectrometric and Molecular Orbital Study, J. Phys. Chem. 100 (1996) 3552–3556.

[3] M. H. Almatarneh, C. G. Flinn, R. A. Poirier, Ab Initio Study of the Deamination of Formamidine, Can. J. Chem. 83 (2005) 2082–2090.

[4] M. H. Almatarneh, C. G. Flinn, R. A. Poirier, W. A. Sokalski, Computational Study of the Deamination Reaction of Cytosine with H_2O and OH^-, J. Phys. Chem. A 110 (2006) 8227–8234.

[5] M. H. Almatarneh, C. G. Flinn, R. A. Poirier, Mechanisms for the Deamination Reaction of Cytosine with H_2O/OH^- and $2H_2O/OH^-$: A Computational Study, J. Chem. Info. Mod. 48 (2008) 831–843.

[6] H. G. Cook, Enamines: Synthesis, Structure, and Reactions, Marcel Dekker, New York, pp 1–102, 1969.

[7] E. M. Kaiser, R. A. Benkeser, Organic Syntheses, Coll. Vol. 6, pp 852–856, 1988.

[8] H. A. Taylor, The Decomposition of Ethylamine. A Unimolecular Reaction, J. Phys. Chem. 34 (1930) 2761–2770.

[9] H. A. Taylor, J. G. Ditman, The Decomposition of Ethylamine and Diethylhydrazine, J. Chem. Phys. 4 (1936) 212–218.

[10] S. Li, D. F. Davidson, R. K. Hanson, Shock Tube Study of Ethylamine Pyrolysis and Oxidation, US National Combustion Meeting 8 (2013), Paper No. 070RK-0075.

[11] A. Lucassen, K. Zhang, J. Warkentin, K. Moshammer, P. Glarborg, P. Marshall, K. Kohse-Höinghaus Fuel-nitrogen conversion in the combustion of small amines using dimethylamine and ethylamine as biomass-related model fuels, Combust. Flame 159 (2012) 2254–2279.

[12] F. J. Lovas, F. O. Clark, E. Tieman, Pyrolysis of ethylamine. I. Microwave spectrum and molecular constants of vinylaminem, J. Chem. Phys. 62 (1975) 1925–1931.

[13] D. E. Gardin, G. A. Somorjai, Vibrational Spectra and Thermal Decomposltlon of Methylamine and Ethylamhe on Ni(III), J. Phys. Chem. 96 (1992) 9424–9431.

[14] U. Mioc, N. Petranovic, Ethylamine behavior of 3A zeolite surface, J. Phys. Chem. 79 (1975) 1476–1478.

[15] K. A. Pearlstine, C. M. Friend, Surface chemistry of alkylamines. 1. Ethylamine and triethylamine on W(100), W(100)-(5.times.1)-C, and W(100)-(2.times.1)-O, J. Am. Chem. Soc. 108 (1986) 5837–5842.

[16] F. Jordan, Nonempirical Molecular Orbital Calculations on the Electronic Structures, Preferred Geometries, and Relative Stabifities of Some $C_2H_6N^+$ Isomeric Ions, J. Phys. Chem. 80(1) (1976) 76–82.

[17] S. Paul, A. K. Ghoshal, B. Mandal, Physicochemical Properties of Aqueous Solutions of 2-(1-Piperazinyl)-ethylamine, J. Chem. Eng. Data 55 (2010) 1359–1363.

[18] I. Stolkin, T. –K. Ha, Hs. H. Günthard, N-methylmethyleneimine and ethylideneimine: Gas- and matrix-infrared spectra, AB initio calculations and thermodynamic properties, Chem. Phys. 21 (1977) 327–347.

[19] R. C. Kumar, J. M. Shreeve, F-Ethylamine and F-ethylimine, J. Am. Chem. Soc. 102 (1980) 4958–4959.

[20] A. Singh, A. Pramanik, G. Das, B. Mondal, Reduction of Coordinated Acetonitrile to Ethylamine in a Ruthenium Complex by p-Phenylenediamine or Hydroquinone, Organometallics 27 (2008) 6403–6404.

[21] Y. Hamada, K. Hashiguchi, A. Y. Hirakawa, M. Tsuboi, M. Nakata, M. Tasumi, S. Kato, K. Morokuma, Vibrational analysis of ethylamines: Trans and gauche forms, J. Mol. Spectrosc. 102 (1983) 123–147.

[22] Y. Hamada, M. Tsuboi, K. Yamanouchi, K. Kuchitzu, J. Mol. Struct. 146 (1986) 253–262.

[23] A. S. Manocha, E. C. Tuazon, W. G. Fateley, J. Phys. Chem. 78 (1974) 803–807.

[24] M. Tsuboi, K. Tamagake, A. Y. Hirakawa, J. Yamaguchi, H. Nakagawa, A. S. Manocha, E. C. Tuazon, W. G. Fateley, Internal rotation in ethylamine: A treatment as a two-top problem, J. Chem. Phys. 63 (1975) 5177–5189.

[25] J. R. Durig, Y. S. Li, Raman spectra of gases. XVIII. Internal rotational motions in ethylamine and ethylamine-d, J. Chem. Phys. 63 (1975) 4110–4113.

[26] J. R. Durig, C. Zhang, T. K. Gounev, W. A. Herrebout, B. J. van der Veken, Conformational Stability From Temperature-Dependent Fourier Transform Infrared Spectra Of Noble Gas Solutions, r_0 Structural Parameters, and Barriers To Internal Rotation for Ethylamine, J. Phys. Chem. A 110 (2006) 5674–5684.

[27] (a) E. Fischer, I. Botskor, The microwave spectrum of trans-ethylamine, J. Mol. Spectrosc. 91 (1982) 116–127. (b) E. Fischer, I. Botskor, The microwave spectrum of gauche-ethylamine, J. Mol. Spectrosc. 104 (1984) 226–247.

[28] L. Radom, W. J. Hehre, J. A. Pople, Molecular orbital theory of the electronic structure of organic compounds. XIII. Fourier component analysis of internal rotation potential functions in saturated molecules, J. Am. Chem. Soc. 94 (1972) 2371–2381.

[29] S. Katsumata, T. Iwai, K. Kimura, Photoelectron Spectra and Sum Rule Consideration. Higher Alkyl Amines and Alcohols, Bull. Chem. Soc. Jpn. 46 (1973) 3391–3395.

[30] R. Maruyama, K. Ohno, Two-Dimensional Penning Ionization Electron Spectroscopy of 2-Aminoethanol and Related Molecules by He*(2^3S) Atoms: Influence of Intramolecular Hydrogen Bonding on Collisional Ionization, J. Phys. Chem A. 108 (2004) 4211–4218.

[31] D. Zeroka, J. O. Jensen, A. C. Samuels, Rotation/Inversion Study of the Amino Group in Ethylamine, J. Phys. Chem. A 102 (1998) 6571–6579.

[32] D. Zeroka, J. O. Jensen, A. C. Samuels, J. Mol. Struct. (THEOCHEM) 456 (1999) 119–126.

[33] M. Yan, X. Shan, F. Wu, X. Xia, K. Wang, K. Xu, X. Chen, Electron Momentum Spectroscopy Study on Valence Electronic Structures of Ethylamine, J. Phys. Chem. A 113 (2009) 507–512.

[34] X. Lu, W. Guo, T. Yang, L. Zhao, S. Du, L. Wang, H. Shan, Gas-Phase Reactions of Co^+ with Ethylamine: A Theoretical Approach to the Reaction Mechanisms of Transition Metal Ions with Primary Amines, J. Phys. Chem. A 112 (2008) 5312–5321.

[35] K. Müller, L. D. Brown, Enamines I. Vinyl Amine, a Theoretical Study of its Structure, electrostatic potential, and proton affinity, Helvetica Chimica Acta 61 (1978) 1407–1418.

[36] R. A. Eades, D. A. Weil, M. R. Ellenberger, W. E. Farneth, D. A. Dixon, C. H. Jr. Douglass, Electronic Structure of Vinylamine. Proton Affinity and Conformational Analysis, J. Am. Chem. Soc. 103 (1981) 5372–5377.

[37] M. J. Frisch, et al. Gaussian03, Revision A.11, Gaussian, Inc.: Pittsburgh, PA, 2001.

[38] (a) C. Lee, W. Yang, R. G. Parr, Development of the Colle-Salvetti correlation-energy formula into a functional of the electron density**,** Phys. Rev. B 37 (1988) 785–789. (b) A. D. Becke, Density-functional thermochemistry. III. The role of exact exchange, J. Chem. Phys. 98 (1993) 5648–5652. (c) A. D. Becke, Density-functional thermochemistry. IV. A new dynamical correlation functional and implications for exact-exchange mixing, J. Chem. Phys. 104 (1996) 1040–1046.

[39] (a) C. Peng, H. B. Schlegel, Combining Synchronous Transit and Quasi-Newton Methods to Find Transition States, Isr. J. Chem. 33 (1993) 449–454. (b) C. Peng, P. Y. Ayala, H. B. Schlegel, M. J. Frisch, Using redundant internal coordinates to optimize equilibrium geometries and transition states, J. Comp. Chem. 17 (1996) 49–56.

[40] D. M. Wardlaw, R. A. Marcus, RRKM reaction rate theory for transition states of any looseness, Chem. Phys. Lett. 110 (1984) 230–234.

[41] V. Mokrushin, V. Bedanov, W. Tsang, M. Zachariah, V. Knyazev, ChemRate; Version1.19[Ed.], NIST: Gaithersburg, 2002.

[42] C. Eckart, The Penetration of a Potential Barrier by Electrons**,** Phys. Rev. 35 (1930) 1303–1309.

[43] T. J. Bevilacqua, R. B. Weisman, Collisional vibrational relaxation of a triplet state: Energy-dependent energy loss from T_1 pyrazine,

J. Chem. Phys. 98 (1993) 6316–6326.

Biographies

Mansour H. Almatarneh obtained his Ph.D. degree in theoretical and computational chemistry from Memorial University in 2007. He was a postdoctoral fellow in the biochemistry department at Memorial University. He was an assistant professor of physical chemistry at Al-Hussein University. He held visiting appointments at Thompson Rivers University and Memorial University in Canada. He is currently an assistant professor at Jubail University College. His research interests are broad throughout reaction mechanisms, medicinal chemistry, biochemistry, ab initio calculations, and molecular dynamics simulations.

Mohammednoor Altarawneh obtained his Ph.D. degree in Chemical Engineering/ Theromdynamics & Reaction Kinetics from University of Newcastle in 2008. He is an associate professor in the Chemical Engineering Department at Al-Hussein Bin Talal University. His research interest is based on the application of quantum chemistry to gain a better insight in chemical reactions.

Raymond A. Poirier is honoured as a 2012 University Research Professor at Memorial University. He is a leading scientist in computational chemistry and fundamental studies of reaction mechanisms. Much of his work is centered on the development of his own quantum chemistry program package, MUNgauss. His area of interest is theoretical/computational chemistry and computational science. He has a very strong publication record that has been cited more than 1,800 times. He has made significant contributions in furthering the understanding of chemistry through the development of theory and computational

Ibrahim A. Saraireh is an associate professor of organic chemistry at Al-Hussein Bin Talal University. He obtained his Ph.D. degree in organic chemistry from University of Jordan in 2005. His research area is synthesis of organic compounds and reaction mechanisms.

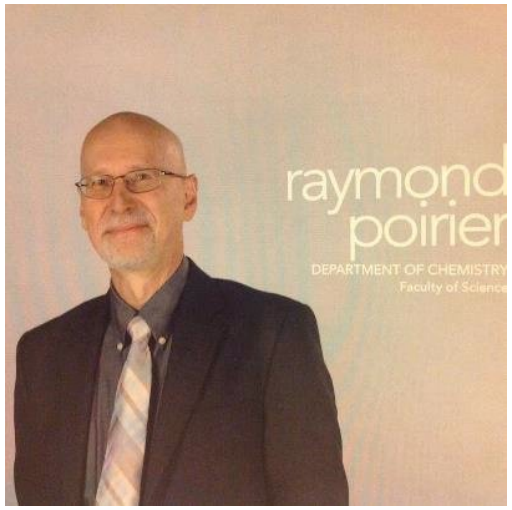

Table 1. Calculated and Experimental Ground-State Geometries and Total Energies for *Trans*- and *Gauche*-Ethylamine (in Hartrees).

Geometrical Coordinate*	*trans*-$CH_3CH_2NH_2$				*gauche*-$CH_3CH_2NH_2$				
	MP2 [a]	**B3LYP [b]**	**Expt'l [c,d]**	**B3LYP [f]**	**MP2 [a]**	**B3LYP [b]**	**MP2 [e]**	**Expt'l [d]**	**B3LYP [f]**
r(C-C)	1.530	1.530	1.525[c], 1.531[d]	**1.535**	1.523	1.522	1.519	1.524	**1.528**
r(C-N)	1.465	1.464	1.477[c], 1.470[d]	**1.468**	1.467	1.466	1.466	1.475	**1.470**
r(C-H)	1.095	1.092	1.092[c], 1.107[d]	**1.098**	1.096	1.090	1.094	1.107	**1.097**
r(N-H)	1.016		1.011[c], 1.052[d]	**1.019**	1.016		1.019	1.052	**1.018**
<CCN	115.3	116.0	114.8[c], 115.0[d]	**116.1**	109.7	110.7	109.8	109.7	**110.5**
< CCH	110.9		111.4[c], 113.2[d]	**111.2**	110.5		110.7	113.2	**110.9**
<CNH	108.8		112.6[c], 111.1[d]	**110.7**	109.1		109.8	112.4	**111.1**
< HNCC	+57.2			**-59.2**	+178.9		-65.6	+180.0	**+64.4**
	+57.2			**+59.1**	+63.8			+59.5	**-177.0**
Total Energy				**-135.179406**					**-135.1792954**

*Bond lengths are in angstroms, and bond angles are in degrees. [a] Ref. 31 (based on MP2/6 311G(d,p) geometries). [b] Ref. 34 based on B3LYP/6-311++G(2df,2pd) geometries. [c] Ref 25 (based on rotational constants of *trans*-CH_3CH_2NH2); [d] Ref. 22 (based on electron diffraction); [e] Ref. 2 (based on MP2/6-31G(d) geometries). [f] This work.

Table 2. Activation Energies and Gibbs Energies of Activation for the Decomposition of Ethylamine in (kJ mol^{-1}) at 298.15 K (Pathways **A→D**).

	HF/ 6-31G(d)	**HF/ 6-31+G(d)**	**MP2/ 6-31G(d)**	**MP2/ 6-31+G(d)**	**B3LYP/ 6-31G(d)**	**B3LYP/ 6-31+G(d)**	**G3MP2**	**G3MP2B3**	**G3B3**
$\Delta E^{\ddagger}, TS_A$	361	348	315	293	294	281	287	285	287
$\Delta G^{\ddagger}, TS_A$	360	347	317	292	294	281	286	285	287
$\Delta E^{\ddagger}, TS_B$	520	516	458	451	426	423	422	422	425
$\Delta G^{\ddagger}, TS_B$	517	513	455	448	423	420	418	419	422
$\Delta E^{\ddagger}, TS_C$	697	695	640	645	569	599	289	548	557
$\Delta G^{\ddagger}, TS_C$	695	693	642	647	564	600	290	543	552
$\Delta E^{\ddagger}, TS_D$	598	579	535	520	492	482	470	471	479
$\Delta G^{\ddagger}, TS_D$	597	578	534	519	491	481	469	469	478

Table 3. The Enthalpies and Gibbs Energies for the Decomposition Reaction of Ethylamine in (kJ mol^{-1}) at 298.15 K for pathways (**A→D**).

	HF/ 6-31G(d)	**HF/ 6-31+(G)**	**MP2/ 6-31G(d)**	**MP2/ 6-31+G(d)**	**B3LYP/ 6-31G(d)**	**B3LYP/ 6-31+G(d)**	**G3MP2**	**G3MP2B3**	**G3B3**
ΔH_A	67	60	75	67	77	63	53	54	56
ΔG_A	45	27	54	40.	50	41	24	26	29
ΔH_B	50	45	57	55	52	54	61	62	63
ΔG_B	11	25	22	39	21	19	21	31	32
ΔH_C	93	94	74	76	81	84	86	87	91
ΔG_C	72	69	54	60	62	68	64	68	72
ΔH_D	126	118	109	104	110	105	101	101	105
ΔG_D	105	93	89	81	93	84	79	83	87

Table 4. Modified Arrhenius Parameters for the High-Pressure limit Reaction Rate Constants for Five Pathways in the Unimolecular Decomposition of Ethylamine (*A* in s^{-1} and *Ea* in J/mol).

Pathway	*A*	*n*	*Ea*
A	3.24×10^{10}	0.98	285 700
B	5.13×10^{10}	1.10	423 700
C	4.17×10^{9}	1.60	548 000
D	1.48×10^{9}	1.52	471 500
E	5.92×10^{12}	1.46	362 200

Table 5. Modified Arrhenius Parameters for the Two Dominating Pathways, ***A*** and ***E***, at Pressures of 0.01 atm, 1.00 atm, and 100.00 atm. (*A* in s^{-1} and *Ea* in J/mol).

Pathway	P (atm)	*A*	*n*	*Ea*
A	0.01	3.46×10^{12}	0.00	280 100
	1.00	1.70×10^{13}	0.00	286 100
	100.00	4.17×10^{13}	0.00	289 600
E	0.01	2.29×10^{14}	0.00	342 000
	1.00	1.67×10^{16}	0.00	356 800
	100.00	1.91×10^{17}	0.00	365 900

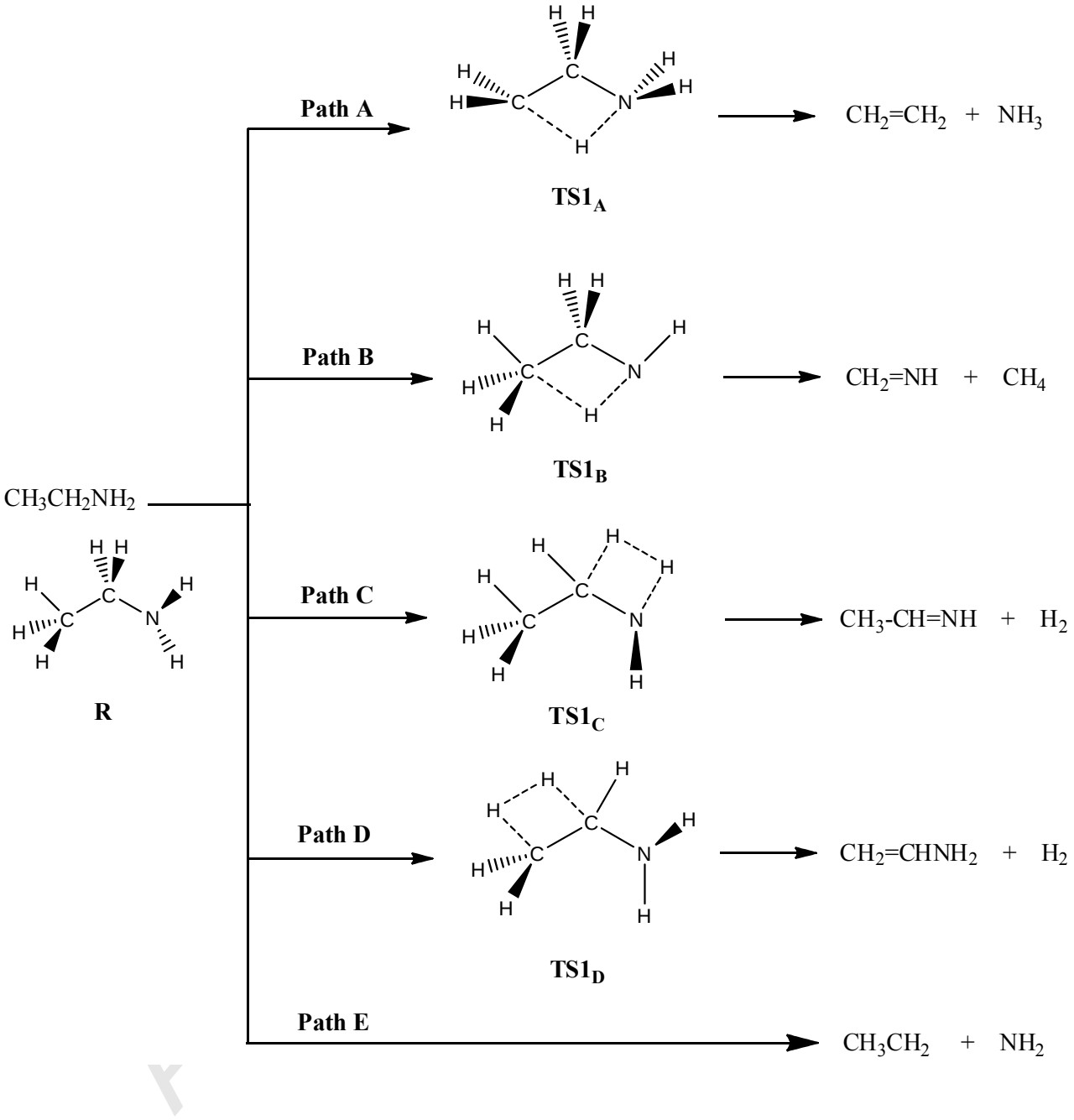

Scheme 1. The Proposed Mechanisms for the Decomposition Reaction of Ethylamine.

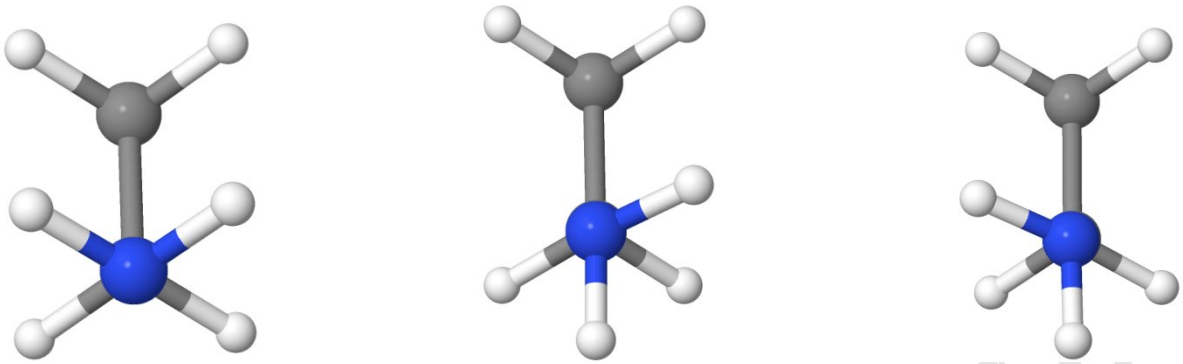

(a) R-*Trans* (b) R-*Gauche* (c) R-*Gauche*

Fig. 1. The B3LYP/631+G(d) optimized ground state geometries for (a) *trans*-ethylamine; (b, c) *gauche*-ethylamine. Hydrogen is white, carbon is gray, and nitrogen is blue.

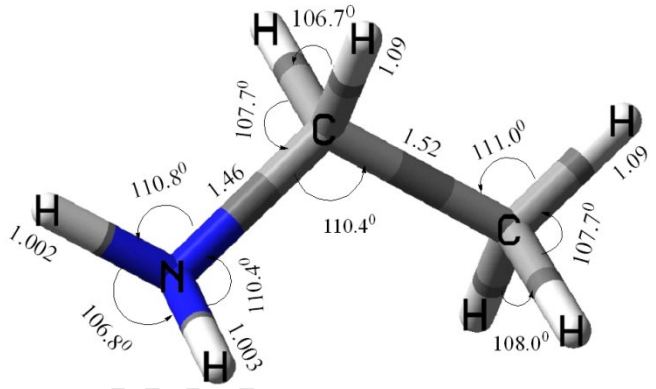

Fig. 2. The optimized geometry of *gauche*-ethylamine. The bond lengths are in Å and bond angles are in degrees. The structural parameters for both conformers are in Table 1.

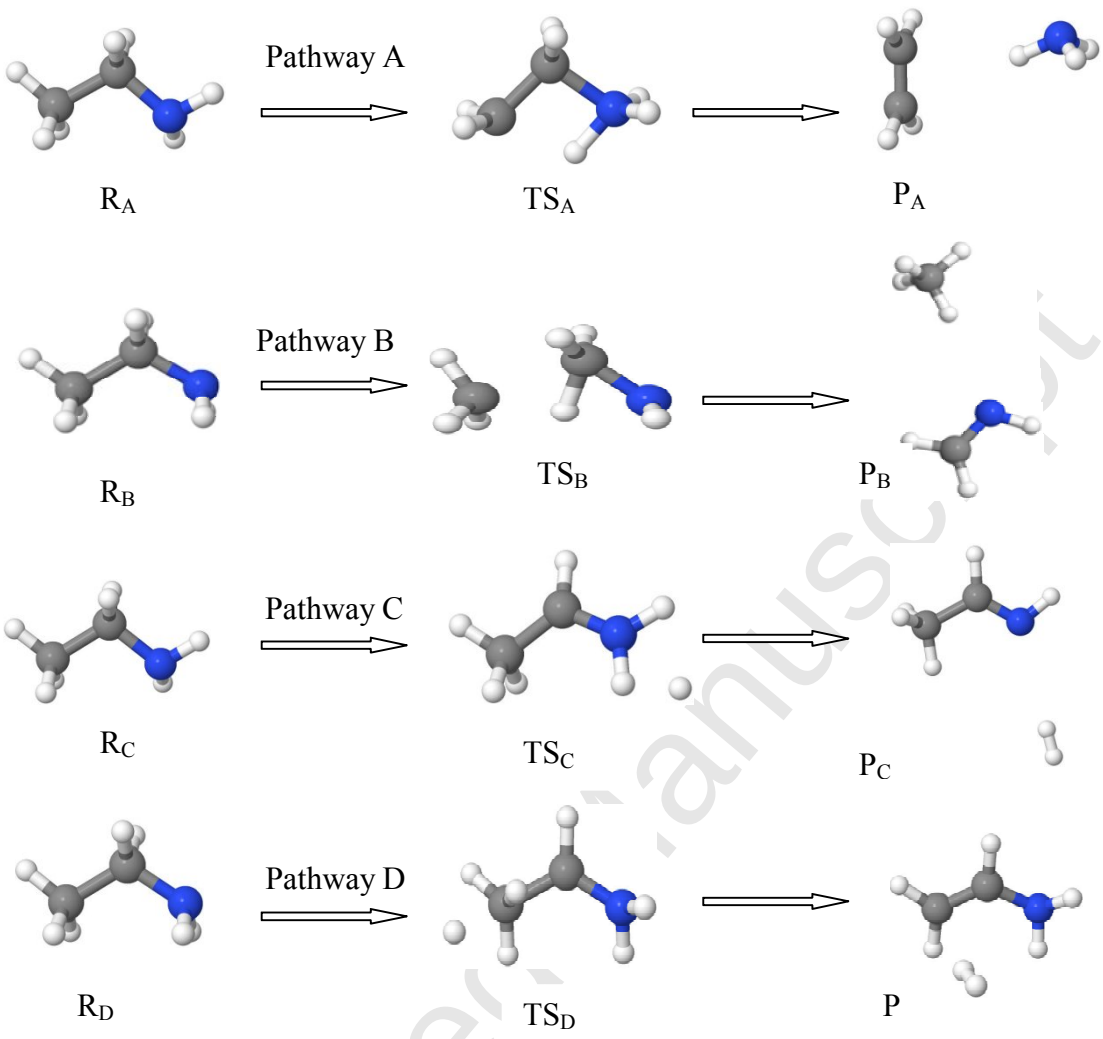

Fig. 3. The optimized structures for all reaction pathways (**A→D**) for the decomposition reaction of ethylamine.

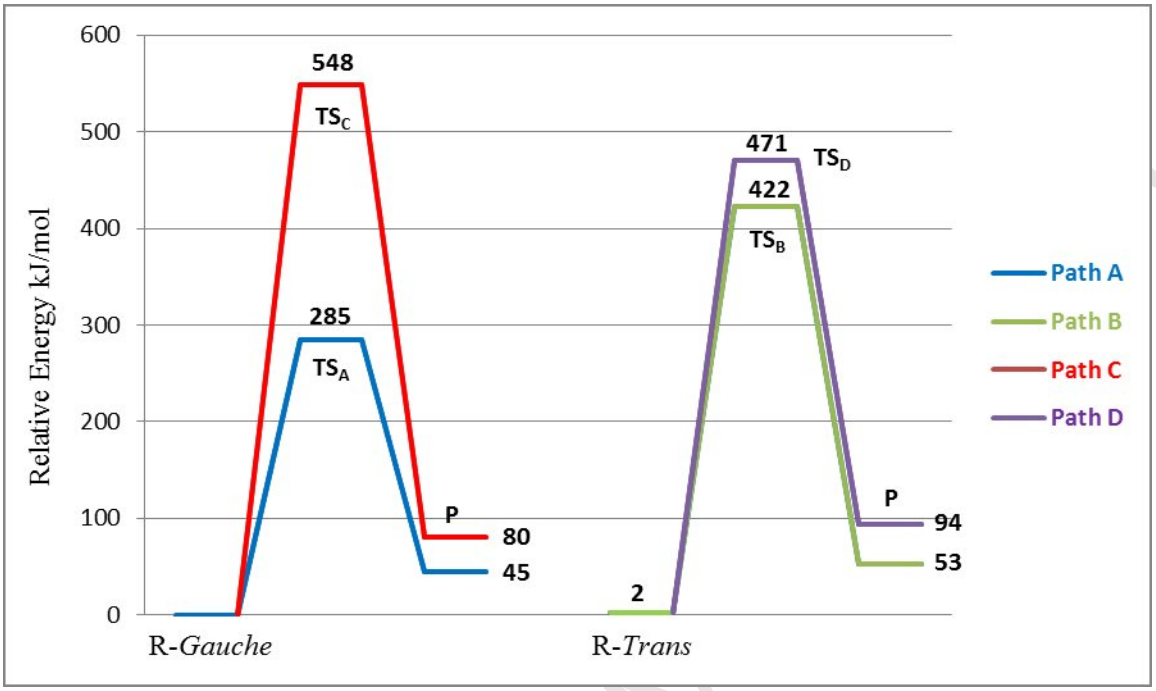

Fig. 4. All reaction pathways (**A→D**) for the decomposition reaction of ethylamine. Relative energies at G3MP2B3 Level of Theory.

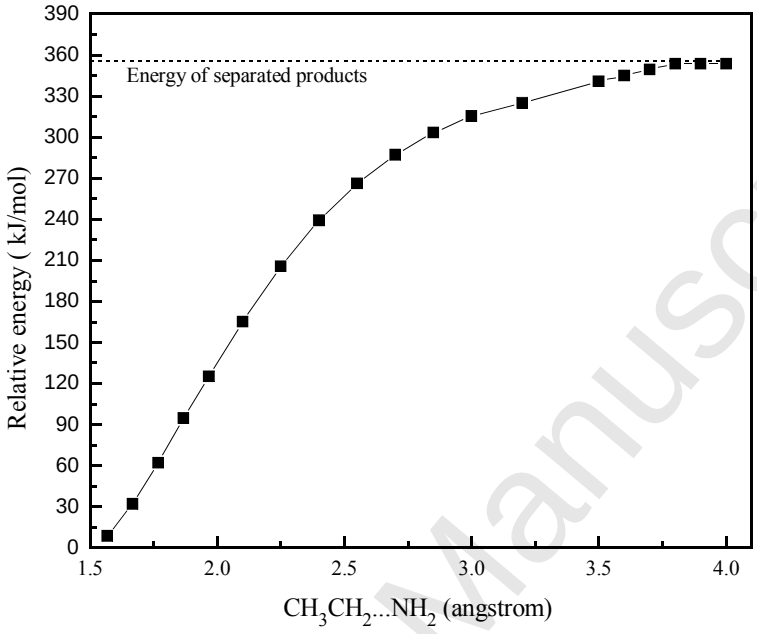

Fig. 5. PES for the CH_3CH_2-NH_2 bond in ethylamine calculated at G3MP2B3.

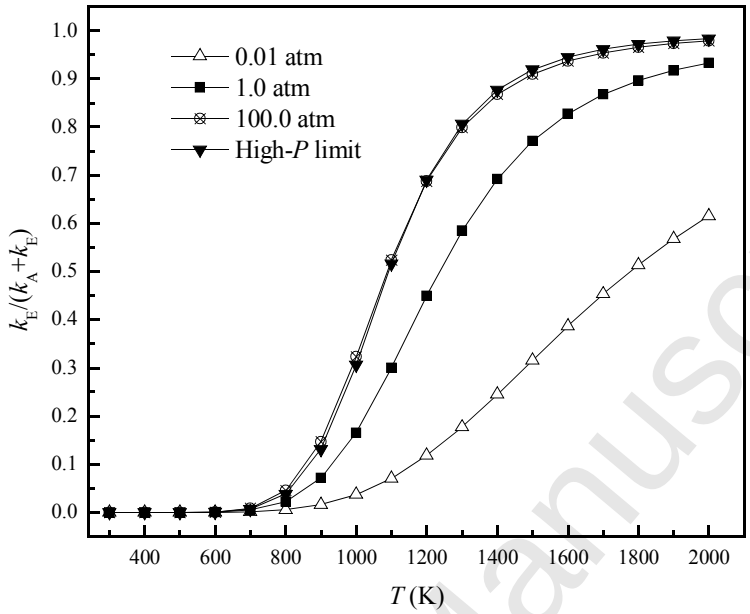

Fig. 6. Plot of pathway **E** branching ratio as a function of temperature for different pressures at the energy transfer value of 800 cm^{-1}.

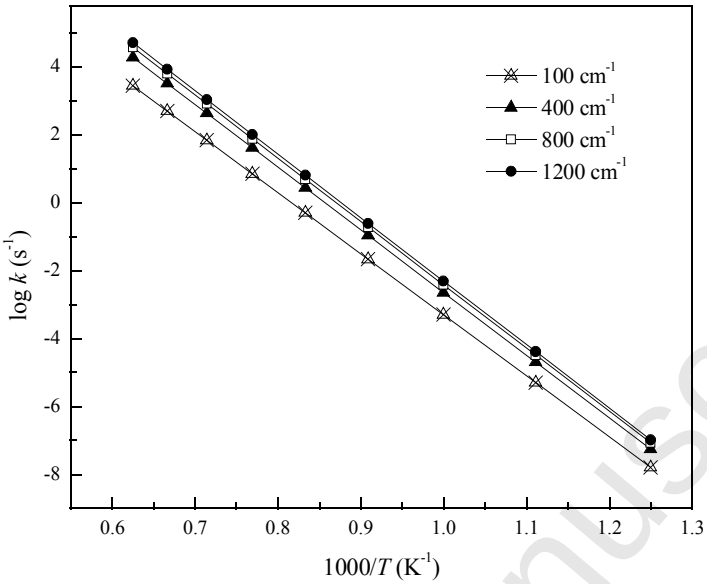

Fig. 7. The effect of $\langle E \rangle_{down}$ on the branching ratio of pathway **A** at 1.0 atm.

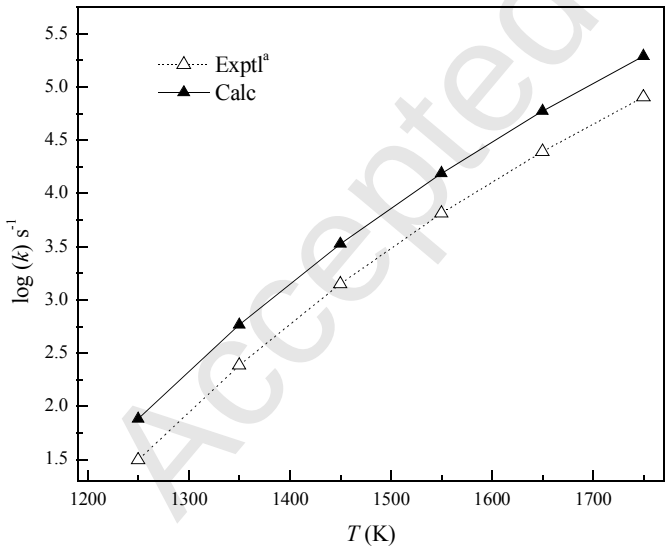

Fig. 8. Comparison between calculated and experimental reaction rate constant for channel **E**. [a] Ref 10